

Mission Analysis for Vesta and Ceres Exploration Using Electric Sail With Classical and Advanced Thrust Models

MINGYING HUO 
SHILEI CAO
YANFANG LIU 

Harbin Institute of Technology, Harbin, China

HE LIAO

Shanghai Institute of Satellite Engineering, Shanghai, China

NAIMING QI 

Harbin Institute of Technology, Harbin, China

The electric sail is an innovative concept for spacecraft propulsion, which can generate continuous thrust without propellant by reflecting solar wind ions. In previous studies, the thrust of an electric sail is described by a classical model that neglects the effects of the electric sail attitude on the propulsive thrust modulus and direction. This paper reappraised the performance of the electric sail in the Vesta and Ceres exploration mission with an advanced thrust model that considers the effect of the spacecraft attitude on both the thrust modulus and direction. By using a hybrid optimization method, the trajectory optimization of the electric-sail-based spacecraft from earth to Vesta and Ceres is implemented in an optimization framework. Numerical results show that the minimal flight time with the advanced thrust model is longer than that with the classical model. The differ-

Manuscript received October 6, 2017; revised September 22, 2018 and December 22, 2018; released for publication December 22, 2018. Date of publication February 11, 2019; date of current version December 5, 2019.

DOI. No. 10.1109/TAES.2019.2897040

Refereeing of this contribution was handled by Z. Davis.

This work was supported in part by the National Science Foundation of China under Grant 11702072, in part by the China Postdoctoral Science Foundation under Grant 2017M611372, in part by the Heilongjiang Postdoctoral Fund under Grant LBH-Z16082, in part by the Open Fund of National Defense Key Discipline Laboratory of Micro-Spacecraft Technology under Grant HIT.KLOF.MST.201607, in part by the Qian Xuesen Laboratory of Space Technology under Grant QXS-ZZJJ-02, and in part by the innovation fund of Harbin Institute of Technology under Grant 30620170018.

Authors' addresses: M. Huo, S. Cao, Y. Liu, and N. Qi are with the Harbin Institute of Technology, Harbin 150001, China, E-mail: (huomingying123@gmail.com; caosl@stu.hit.edu.cn; liu-yanfang@hotmail.com; qin-mok@163.com); H. Liao is with the Shanghai Institute of Satellite Engineering, Shanghai 201109, China, E-mail (liaohe_crane@163.com). (Corresponding author: Mingying Huo.)

0018-9251 © 2019 OAPA

ence in performance between the classical and advanced models is attributable to overestimation of the maximum thrust cone angle and the thrust modulus by the classical model.

I. INTRODUCTION

The electric solar wind sail (electric sail for short) is an innovative concept for spacecraft propulsion that was first proposed in 2004 [1]. As shown in Fig. 1, the electric sail consists of thin centrifugally stretched tethers charged by an onboard electron gun. Through the interaction of the artificial electric field generated by the tethers, the electric sail deflects proton flow in solar winds to generate a propulsive thrust. Similar to solar sails, electric sails can produce continuous thrust without the need for propellant. However, unlike solar sails, electric sails are propelled by the solar wind dynamic pressure instead of the solar photon momentum. Over the years, the electric sail concept has been investigated by means of laboratory tests and plasma-dynamic simulations [2]–[4]. A prototype of an electric sail, called Aalto-1 CubeSat [5], [6], was launched into low earth orbit (LEO) on June 23, 2017. At present, the readiness of the plasma brake has been confirmed in the Aalto-1 mission, and it will be used near the end of the mission when deorbiting of the satellite starts later in 2018.

The electric sail has received increased interest in the past years. In particular, much effort has been devoted to the study of a mathematical model that can accurately estimate the propulsive acceleration of the electric sail and is sufficiently simple to be used within a preliminary mission analysis. Over the years, the mathematical thrust model of the electric sail has undergone important changes. From a historical viewpoint, Janhunen and Sandroos [7] first proposed a thrust model in 2007. Their proposed model provides a purely radial thrust that varies with the Sun-spacecraft distance as $r^{7/6}$. Based on this, Mengali *et al.* [8] proposed a mathematical model for the propulsive thrust that takes into account the possibility of generating an off-radial propulsive acceleration. The off-radial component of the propulsive acceleration can be obtained by changing the pitch angle α_n , which is defined as the angle between the radial direction and that of a unit vector normal to the plane in the direction opposite to the sun. A maximum thrust cone angle α_{\max} of approximately 30° – 35° was assumed in order to prevent possible occurrence of mechanical instabilities of the electric sail associated with a high value of the sail pitch angle (i.e., α_n greater than approximately 60° – 70°). Using more advanced plasma dynamic simulations, Janhunen showed that the variation of the propulsive acceleration modulus is inversely proportional to the distance from the sun [9], [10].

In the earlier reports, the effects of the attitude of the electric sail on the propulsive thrust modulus and direction were neglected. The thrust modulus was assumed to be invariable with the change in the pitch angle, and the thrust cone angle was assumed to be approximately equal to one-half of the pitch angle. Obviously, the above models are not accurate enough to describe the thrust vector of an electric sail for current mission analysis. In our previous research

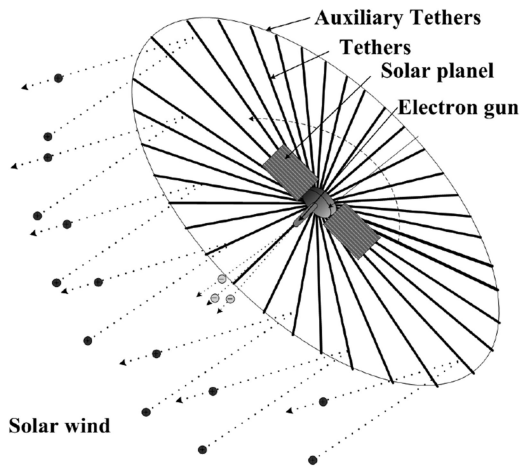


Fig. 1. Conceptual sketch of an electric sail.

[11], a mathematical model characterizing the propulsive thrust of the electric sail was described as a function of the orbital radius and three Euler angles. However, the influence of pitch angle on thrust modulus and thrust cone angle was not discussed. With the aid of recent numerical and experimental data, Yamaguchi and Yamakawa proposed an advanced thrust model of the electric sail in the form of polynomial fitting [12]. In this advanced thrust model, the thrust modulus and thrust cone angle were described as polynomial functions of the pitch angle based on numerical and experimental data. Using the polynomial fitting model proposed by Yamaguchi and Yamakawa, Mengali and Quarta [13] obtained a series of minimum-time trajectories of the electric sail for a classical circle-to-circle coplanar heliocentric orbit transfer to review the different thrust models. Furthermore, an advanced thrust model of the electric sail in analytical form was introduced in [14]. This model considered the effect of the spacecraft attitude on both the thrust modulus and direction.

In this paper, direct comparisons of the classical thrust model [9], [10], polynomial-fitting thrust model [12], and analytical thrust model [14] are made, in order to reanalyze the propulsion performance of the electric sail. In addition, an interesting mission scenario—specifically, a tour from earth to Vesta and Ceres—is analyzed to discuss the possibility of using electric sails in this mission scenario. Vesta and Ceres were chosen as two contrasting protoplanets, the former is apparently “dry” (i.e., rocky) whereas the latter is “wet” (i.e., icy). Exploration of Vesta and Ceres can provide a bridge in scientific understanding between the formation of rocky planets and icy bodies, which is of great significance when considering the formation of the solar system. This selected mission scenario is similar to Dawn [15], which is a space probe launched by NASA in September 2007. Dawn is the first spacecraft to orbit two extraterrestrial bodies, the first spacecraft to visit either Vesta or Ceres, and the first to visit a dwarf planet, arriving at Ceres in March 2015. Dawn entered Vesta orbit on July 16, 2011 and completed approximately a one-year survey mission before leaving for Ceres in 2012. Dawn entered Ceres orbit

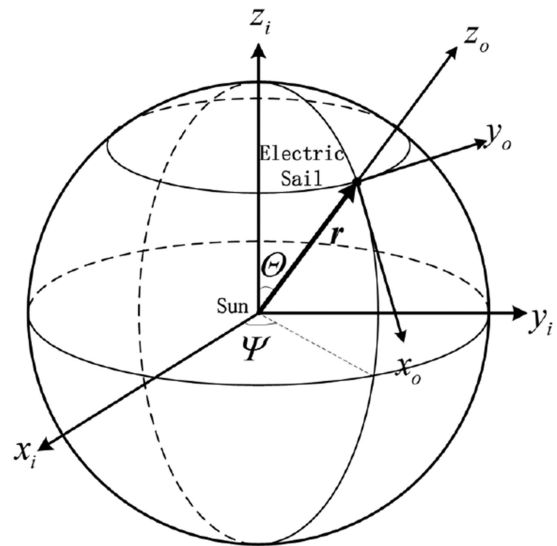


Fig. 2. Orbital reference frame and heliocentric-ecliptic frame.

on March 6, 2015 [16], and is predicted to remain in orbit perpetually after concluding its mission.

In this paper, this mission scenario is analyzed within an optimal framework by using a hybrid direct optimization method [17], which combines a genetic algorithm (GA) and the Gauss pseudospectral method (GPM) [18]. The GA is used to conduct a random search within the space of feasible solutions and provide a reasonable initial guess for the state and control histories used in nonlinear programming (NLP) problems, which is transcribed from the continuous optimal control problem by using GPM. This hybrid optimization method is capable of searching the feasible and optimal solutions space without any initial value guess. This feature is ideal for the trajectory optimization problem in this mission scenario, for which there is generally no prior knowledge of the initial time and state vector. A detailed description of the hybrid algorithm can be found in [17].

The remainder of the paper is organized as follows. Section II compares the classical thrust model, polynomial-fitting thrust model, and analytical thrust model. Section III describes the trajectory problem of the mission scenario from earth to Vesta and Ceres with the analytical thrust model. Section IV presents numerical results within an optimal framework, and these results are used to reanalyze the propulsion performance of the electric sail. Section V presents concluding remarks.

II. COMPARISON OF THRUST MODELS OF ELECTRIC SAIL

A. Reference Frames

To describe the thrust model and the orbit dynamics of the electric sail, the orbital reference frame $o_o x_o y_o z_o$ and the heliocentric-ecliptic inertial frame $o_i x_i y_i z_i$ are introduced as illustrated in Fig. 2. The origin o_o of the orbital frame is defined at the center-of-mass of the electric-sail-based spacecraft. The z_o -axis is defined along the sun-spacecraft direction, which coincides with the approximate direction

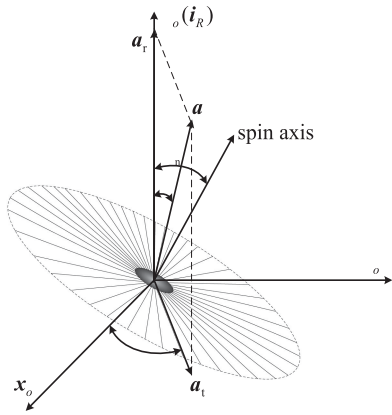


Fig. 3. Pitch angle α_n and clock angle δ .

of propagation of the solar wind. The y_o -axis is perpendicular to the z_o -axis and the normal of the ecliptic plane, and the x_o -axis forms a right-handed triad. The heliocentric-ecliptic inertial frame is defined as follows. The origin o_i is defined at the center-of-mass of the sun, and the x_i -axis is defined in the direction of the sun equinox. The z_i -axis is along the normal of the ecliptic plane and the direct north ecliptic pole. The y_i -axis forms a right-handed system.

In the preliminary mission analysis of the electric sail, the vector of thrust acceleration is usually described by the pitch angle α_n and clock angle δ [13]. As shown in Fig. 3, the pitch angle $\alpha_n \in [0, \pi]$ is the sail nominal plane's inclination angle, and the clock angle $\delta \in [0, 2\pi]$ is the angle between the x_o -axis and the component vector of thrust in the $o_o x_o y_o$ plane. The thrust cone angle α is defined as the angle between the direction vector of thrust acceleration and the direction vector of solar wind velocity (z_o -axis).

B. Classical Thrust Model

As illustrated in Fig. 3, the vector of the electric sail propulsive acceleration in the orbital reference frame $o_o x_o y_o z_o$ can be given as

$$\mathbf{a} = a_c \tau \gamma \left(\frac{r_\oplus}{r} \right) \begin{bmatrix} \sin \alpha \cos \delta \\ \sin \alpha \sin \delta \\ \cos \alpha \end{bmatrix} \quad (1)$$

where r is the distance between the sun and the spacecraft, and r_\oplus is the average distance between the sun and the earth, and a_c is the characteristic acceleration of the electric sail, which is the maximum acceleration when the sun-spacecraft distance $r = r_\oplus$ and the direction of solar wind velocity are perpendicular to the sail plane $\alpha_n = 0^\circ$. $\tau \in [0, 1]$ is the thrust coefficient, which can be adjusted by an electron gun. $\gamma \in [0, 1]$ is the dimensionless acceleration, defined in [12] and [13], which is used to characterize the effect of sail attitude on the modulus of thrust acceleration.

In the classical model, the effects of the electric sail attitude on the propulsive thrust modulus and direction are neglected—the thrust modulus is assumed to be invariable with varying attitude, and the thrust cone angle is assumed to be approximately equal to one-half of the pitch angle. The

TABLE 1
Interpolation Coefficients of Thrust Parameters

k	b_k	c_k
0	0.000	1.000
1	4.853×10^{-1}	6.904×10^{-5}
2	3.652×10^{-3}	-1.271×10^{-4}
3	-2.661×10^{-4}	7.027×10^{-7}
4	6.322×10^{-6}	-1.261×10^{-8}
5	-8.295×10^{-8}	1.943×10^{-10}
6	3.681×10^{-10}	-5.896×10^{-13}

thrust cone angle α_{cla} and the dimensionless acceleration γ_{cla} in the classical thrust model are defined as

$$\alpha_{\text{cla}} = \alpha_n / 2 \quad (2)$$

$$\gamma_{\text{cla}} = 1. \quad (3)$$

C. Polynomial Fitting Thrust Model

For the sake of completeness, the polynomial-fitting thrust model of the electric sail obtained in [12] and [13] is illustrated in this section. With the aid of recent numerical and experimental data, the thrust cone angle α and the dimensionless acceleration γ can be written as polynomial fitting functions of the pitch angle α_n as follows:

$$\alpha_{\text{pol}} = b_6 \alpha_n^6 + b_5 \alpha_n^5 + b_4 \alpha_n^4 + b_3 \alpha_n^3 + b_2 \alpha_n^2 + b_1 \alpha_n + b_0 \quad (4)$$

$$\gamma_{\text{pol}} = c_6 \alpha_n^6 + c_5 \alpha_n^5 + c_4 \alpha_n^4 + c_3 \alpha_n^3 + c_2 \alpha_n^2 + c_1 \alpha_n + c_0 \quad (5)$$

where the coefficients b_k with $k = 0, 1, \dots, 6$ and c_k with $k = 0, 1, \dots, 6$ are given in Table 1.

D. Analytical Thrust Model

As discussed in our recent research [14], an analytical thrust model of the electric sail is proposed, which gives a compact vectorial description of the propulsive acceleration of the electric sail. In the analytic thrust model, the propulsive acceleration of the electric sail takes into account the thrust contribution generated by a single tether. Further, α_{ana} and γ_{ana} can be written as the analytical functions of the pitch angle α_n

$$\alpha_{\text{ana}} = \cos^{-1} \frac{\cos^2 \alpha_n + 1}{\sqrt{3 \cos^2 \alpha_n + 1}} \quad (6)$$

$$\gamma_{\text{ana}} = \frac{1}{2} \sqrt{3 \cos^2 \alpha_n + 1}. \quad (7)$$

E. Comparison of Thrust Cone Angle

To reanalyze the propulsion performance of the electric sail, direct comparisons of the classical thrust model, polynomial-fitting thrust model, and analytical thrust model are implemented in this section. As shown in Fig. 4, the variation of the thrust cone angles α described in the analytical advanced thrust model and in the polynomial-fitting advanced thrust model are in perfect agreement. This can be seen as a mutual corroboration between the two advanced thrust models (polynomial-fitting thrust model and analytical thrust model). Compared to the classical thrust model,

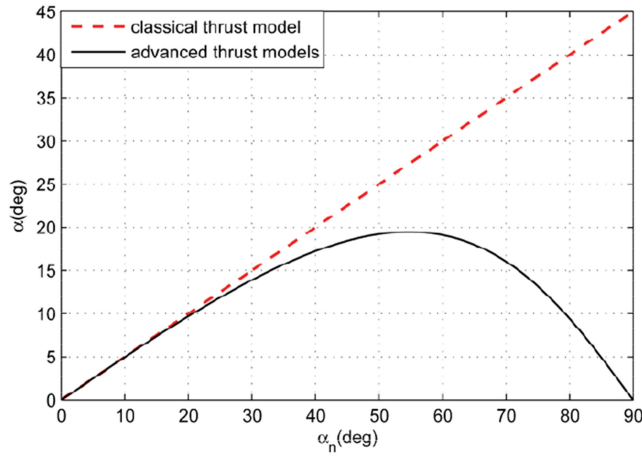


Fig. 4. Comparison of thrust cone angle α .

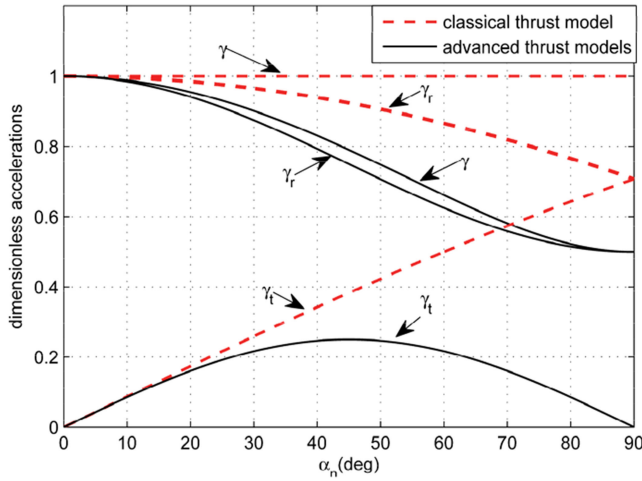


Fig. 5. Comparison of dimensionless accelerations.

the linear variation of the thrust cone angle in the advanced thrust models with the pitch angle in the form $\alpha \simeq \alpha_n/2$ is in good agreement with the classical model until $\alpha_n \leq 20^\circ$. When $\alpha_n > 20^\circ$, the functions $\alpha = \alpha(\alpha_n)$ in the advanced thrust model have a marked nonlinear behavior. It reaches a maximum value $\alpha_{\max} = 19.47^\circ$ at $\alpha_n = 54.75^\circ$, and then it decreases quickly and goes to zero at $\alpha_n = 90^\circ$.

F. Comparison of Dimensionless Acceleration

As shown in Fig. 5, the variations of the dimensionless acceleration γ described in the polynomial-fitting thrust model and analytical thrust model are also in perfect agreement. Compared to the classical thrust model, the dimensionless propulsive accelerations in the advanced thrust models reach their maximum value ($\gamma_{\max} = 1$) at $\alpha_n = 0^\circ$ when the Sun–spacecraft line is normal to the nominal plane of the electric sail. Then, the dimensionless propulsive acceleration decreases monotonically with α_n until it reaches a minimum value $\gamma_{\min} = 0.5$ at $\alpha_n = 90^\circ$. In addition, the radial component and the tangential component of the dimensionless acceleration are always lower in the advanced thrust model than in the classical model. This indicates

that the thrust-invariance assumption in the classical thrust model is not reasonable, and overestimated the radial and tangential thrust accelerations.

III. OPTIMIZATION PROBLEM DESCRIPTION

A. Orbital Dynamics With Analytical Model

The equations of motion for an electric-sail-based spacecraft in a heliocentric ecliptic inertial reference frame $o_i x_i y_i z_i$ can be written as

$$\dot{\mathbf{r}} = \mathbf{v} \quad (8)$$

$$\dot{\mathbf{v}} = -\frac{\mu_s}{r^3} \mathbf{r} + [\mathbf{a}]_{o_i x_i y_i z_i} \quad (9)$$

where μ_s is the sun's gravitational parameter, $\mathbf{r} = [r_x \ r_y \ r_z]^T$ is the spacecraft position vector as seen in Fig. 2, $r = \|\mathbf{r}\| = \sqrt{r_x^2 + r_y^2 + r_z^2}$ is the modulus of the position vector, $\mathbf{v} = [v_x \ v_y \ v_z]^T$ is the spacecraft velocity vector, $[\mathbf{a}]_{o_i x_i y_i z_i}$ is the propulsive acceleration vector described in the heliocentric ecliptic inertial reference frame $o_i x_i y_i z_i$. According to (5)–(7), $[\mathbf{a}]_{o_i x_i y_i z_i}$ can be written as

$$[\mathbf{a}]_{o_i x_i y_i z_i} = \frac{a_c \tau}{2} \left(\frac{r_\oplus}{r} \right) \begin{bmatrix} \cos \Psi & -\sin \Psi & 0 \\ \sin \Psi & \cos \Psi & 0 \\ 0 & 0 & 1 \end{bmatrix} \cdot \begin{bmatrix} \cos \Theta & 0 & \sin \Theta \\ 0 & 1 & 0 \\ -\sin \Theta & 0 & \cos \Theta \end{bmatrix} \cdot \begin{bmatrix} \cos \alpha_n \sin \alpha_n \cos \delta/2 \\ \cos \alpha_n \sin \alpha_n \sin \delta/2 \\ (\cos^2 \alpha_n + 1)/2 \end{bmatrix} \quad (10)$$

where Ψ is the ecliptic longitude and Θ is the ecliptic latitude as shown in Fig. 2. Considering the following geometric relationships:

$$\begin{aligned} \sin \Theta &= \sqrt{r_x^2 + r_y^2}/r & \cos \Theta &= r_z/r \\ \sin \Psi &= r_y/r & \cos \Psi &= r_x/r \end{aligned} \quad (11)$$

the electric-sail-based spacecraft equations of motion can be written in a compact form as

$$\dot{\mathbf{x}}(t) = \mathbf{f}(\mathbf{x}, \mathbf{u}, t) \quad (12)$$

where $\mathbf{x} = [r_x \ r_y \ r_z \ v_x \ v_y \ v_z]^T$ is the state vector, and $\mathbf{u} = [\alpha_n \ \delta \ \tau]^T$ is the control vector.

B. Optimization Problem Description

The trajectory optimization of the mission scenario from earth to Vesta and Ceres was investigated using the following assumptions. The electric-sail-based spacecraft left earth orbit at initial time t_0 with zero hyperbolic excess velocity with respect to the earth, and completed the rendezvous with Vesta at time t_1 . After the flyby with Vesta within a period of time, the spacecraft left Vesta orbit at time t_2 with zero hyperbolic excess velocity, and arrived at Ceres at time t_3 . The optimal control law, that is the time history

of the triplet $\mathbf{u} = [\alpha_n \ \delta \ \tau]^T$, is found by minimizing the total flight time necessary to perform rendezvous with the target planets (Vesta and Ceres). The objective function to be minimized can be written as

$$J = \Delta t_1 + \Delta t_2 + \Delta t_3 \quad (13)$$

where $\Delta t_1 = t_1 - t_0$ is the transfer time from earth to Vesta. $\Delta t_2 = t_2 - t_1 \in [\Delta t_{2\min}, \infty]$ is the flyby time with Vesta, wherein $\Delta t_{2\min}$ is selected as one year in this paper. $\Delta t_3 = t_3 - t_2$ is the transfer time from Vesta to Ceres. The initial time t_0 and flight times $\Delta t_1, \Delta t_2, \Delta t_3$ are design variables optimized in the optimization procedure.

The optimal control law must take into account both the initial condition and the final rendezvous condition, which can be given in (14) as shown at the bottom of this page, where \mathbf{x}_E is the state vector of earth, \mathbf{x}_V is the state vector of Vesta, and \mathbf{x}_C is the state vector of Ceres.

IV. TRAJECTORY OPTIMIZATION AND NUMERICAL RESULTS

This section reappraises the performance of the electric-sail-based spacecraft in an interesting interplanetary transfer to protoplanets (Vesta and Ceres) using the analytical advanced thrust model. In particular, the optimal analysis allows a minimum transfer time to be found (using a hybrid direct optimization method [17]) as a function of the characteristic acceleration a_c using a realistic set of planetary ephemeris data within a time range of 20 years (January 1, 2017 to December 31, 2036). All of the test cases were executed in MATLAB R2012b on a Core i5 Dual-Core 2.20 GHz computer running Windows 10.

A. Case Studies

In general, the value of a_c depends on the payload mass and the technological characteristics of the electric sail, such as the number of tethers and their length. For example, using the parametric mass budget model described in [19], a spacecraft with a total mass of 487 kg and a payload mass of 100 kg, propelled by an electric sail with 44 tethers (of length = 15.4 km each), is able to produce a characteristic acceleration of approximately 0.8 mm/s². Numerical results in [19] show that the electric sail propulsion system could be an interesting option for a wide class of deep space missions that require a characteristic acceleration of up to approximately 3 mm/s². Moreover, some rather straightforward near-term component-level improvements have the potential of reducing the effective mass of the electric sail further (28% in a specific case) with a consequent improve-

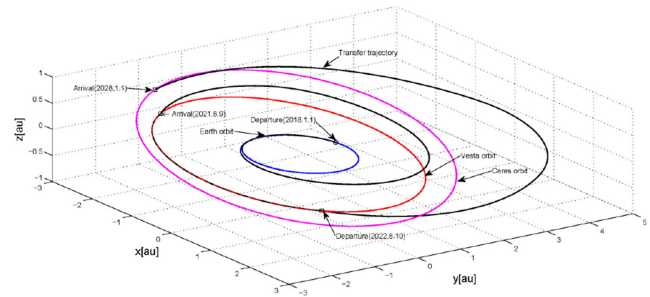


Fig. 6. Trajectories from earth to Vesta and Ceres with advanced thrust model ($a_c = 0.8 \text{ mm/s}^2$).

ment. Therefore, the selected characteristic acceleration ($a_c = 0.8 \text{ mm/s}^2$) in this case is reasonable for the near future.

In this paper, the problem is parameterized as a function of the value of the spacecraft characteristic acceleration, and the simulation results for a mission scenario in which $a_c = 0.8 \text{ mm/s}^2$ are presented. Assuming an optimal earth–Vesta–Ceres transfer with a spacecraft characteristic acceleration of 0.8 mm/s², the transfer trajectory is illustrated in Fig. 6. If the electric-sail-based spacecraft left the sphere of influence of Earth on January 1, 2018 with zero hyperbolic excess velocity, it will take 1317 days to transfer from earth to Vesta. After a one-year observation, the spacecraft left Vesta with zero hyperbolic excess velocity. It will take 1970 days to get into the sphere of influence of Ceres. The total flight time for earth–Vesta–Ceres exploration, propelled by an electric sail with characteristic acceleration of 0.8 mm/s² is 3652 days, which is longer than that of the Dawn spacecraft (about 2750 days). The main reason for this is that the thrust cone angle of the electric sail cannot be adjusted arbitrarily ($\alpha_{\max} = 19.47^\circ$). In contrast, the Dawn spacecraft is propelled by three xenon ion thrusters to generate the required thrust, and also was accelerated through a gravity assist flyby of Mars in 2009. However, note that the Dawn spacecraft exhausted virtually all on-board propellants (425 kg xenon) when it arrived at Ceres, such that it could not continue on to explore other targets. On the other hand, electric sails can produce continuous thrust without the need for propellant, which is meaningful for subsequent exploration of more targets.

Figs. 7 and 8 show the three components of the position and velocity vectors (in the inertial reference frame) for the spacecraft. The time histories of the control angles and thrust coefficient are illustrated in Figs. 9 and 10, respectively. It is worth noting that the existence of three coasting arcs in the optimal trajectory, which do not include with

$$\begin{cases} \mathbf{x}(t_0) = \mathbf{x}_E(t_0) = [r_{xE}(t_0) & r_{yE}(t_0) & r_{zE}(t_0) & v_{xE}(t_0) & v_{yE}(t_0) & v_{zE}(t_0)]^T \\ \mathbf{x}(t_1) = \mathbf{x}_V(t_1) = [r_{xV}(t_1) & r_{yV}(t_1) & r_{zV}(t_1) & v_{xV}(t_1) & v_{yV}(t_1) & v_{zV}(t_1)]^T \\ \mathbf{x}(t_2) = \mathbf{x}_V(t_2) = [r_{xV}(t_2) & r_{yV}(t_2) & r_{zV}(t_2) & v_{xV}(t_2) & v_{yV}(t_2) & v_{zV}(t_2)]^T \\ \mathbf{x}(t_3) = \mathbf{x}_C(t_3) = [r_{xC}(t_3) & r_{yC}(t_3) & r_{zC}(t_3) & v_{xC}(t_3) & v_{yC}(t_3) & v_{zC}(t_3)]^T \end{cases} \quad (14)$$

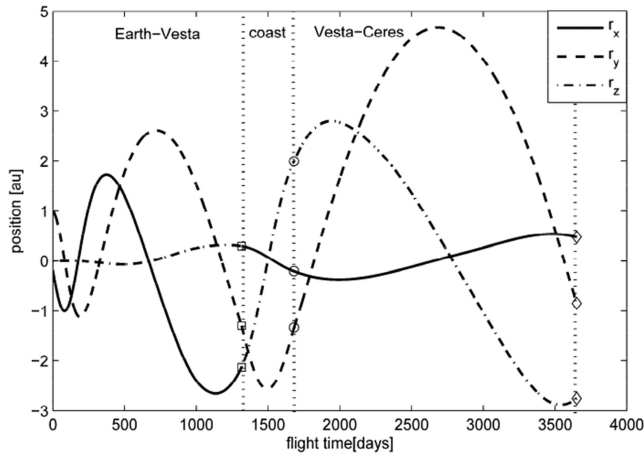


Fig. 7. Position from earth to Vesta and Ceres with the advanced thrust model ($a_c = 0.8 \text{ mm/s}^2$).

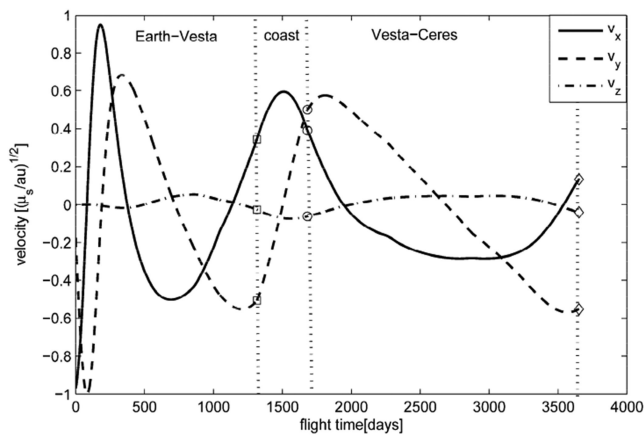


Fig. 8. Velocity from earth to Vesta and Ceres with the advanced thrust model ($a_c = 0.8 \text{ mm/s}^2$).

the coasting arc corresponding to the flyby with Vesta. In addition, the command attitude angle histories generated by the hybrid optimization method is smooth and continuous. Based on the obtained pitch angle α_n , the histories of the cone angle α can be obtained and illustrated as shown in Fig. 9. In the middle of the two transfer processes, the thrust cone angle α maintains the maximum value of 19.47° corresponding to the pitch angle $\alpha_n = 54.75^\circ$.

B. Comparison of Flight Time

To reappraise the performance of an electric-sail-based spacecraft with the analytical advanced thrust model, the trajectory optimizations with the classical thrust model were also implemented as a contrastive reference. When the characteristic acceleration is varied in the range $a_c \in [0.8, 5] \text{ mm/s}^2$, the optimal flight times of the electric-sail-based spacecraft with the analytical advanced thrust model and the classical model are summarized in Fig. 11, which shows an increase in the transfer times as expected when the value of a_c is reduced. In addition, the transfer time using the electric sail with the advanced model is longer than that with the classical model. The difference in performance

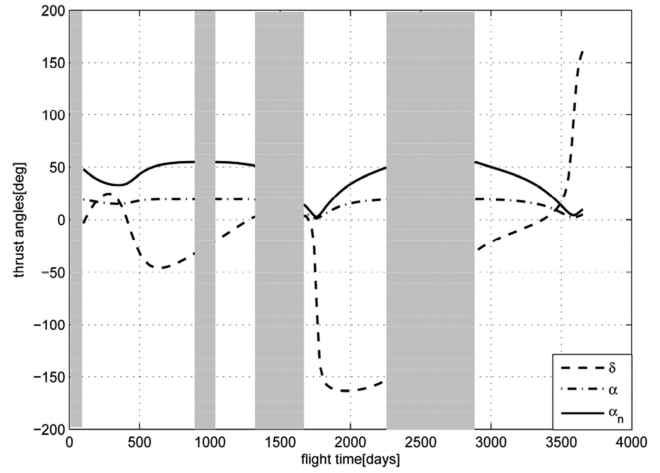


Fig. 9. Thrust angles from earth to Vesta and Ceres with the advanced thrust model ($a_c = 0.8 \text{ mm/s}^2$).

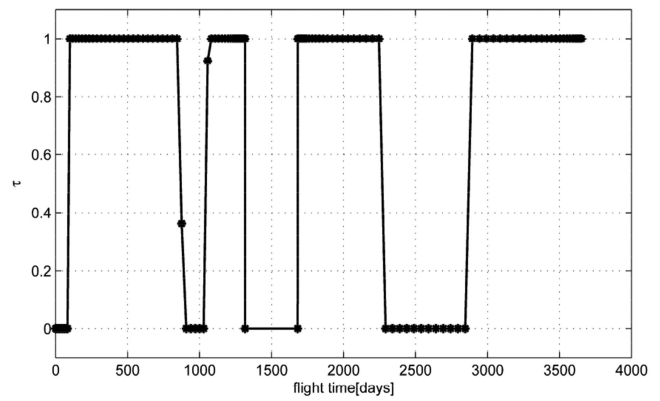


Fig. 10. Thrust coefficient from earth to Vesta and Ceres with the advanced thrust model ($a_c = 0.8 \text{ mm/s}^2$).

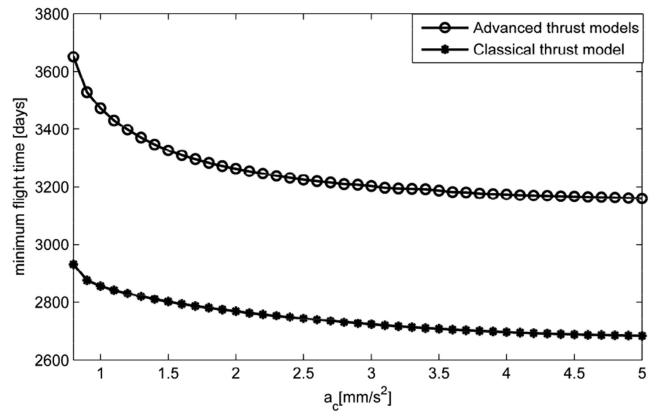


Fig. 11. Minimum transfer time as a function of characteristic acceleration a_c .

between the classical and advanced models is attributable to overestimation of the maximum thrust cone angle and the thrust modulus by the classical model. In the classical thrust model, the maximum thrust cone angle α_{\max} of the electric sail is estimated to be in the range $30^\circ\text{--}35^\circ$, and the effects of the electric sail attitude on the thrust modulus are neglected. However, in the advanced thrust models, the

maximum thrust cone angle α_{\max} of the electric sail is calculated to be approximately equal to 19.5° , and the thrust modulus decreases when the pitch angle α_n varies from 0° to 90° .

Under the same termination conditions for optimization procedures (the convergence criteria for the NLP are a maximum constraint violation of 1×10^{-9} and a reduction in the cost function of less than 1×10^{-6} for one iteration) with the same number of optimized variables and constraints, the average computation time (the average number of required iterations) for generating the optimal trajectory of electric sail with advanced thrust model is about 30% longer (26% larger) than that with classical thrust model. This illustrates that the actual problem is more difficult to be solved because the thrust components in the advanced thrust model are less than those in the classical thrust model.

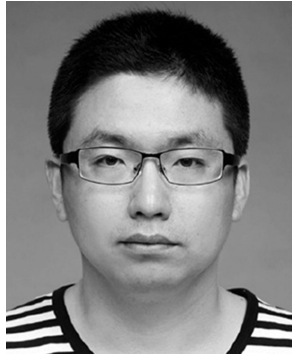
V. CONCLUSION

In this paper, an advanced thrust model of an electric sail in analytical form that considers the effect of the spacecraft attitude on both the thrust modulus and direction, and which was proposed in our previous research, was discussed. To reanalyze the propulsion performance of the electric sail, direct comparisons of the classical thrust model, polynomial-fitting thrust model, and analytical thrust model were carried out. Numerical results showed that the variation of the thrust cone angle α and dimensionless acceleration γ described in the analytical thrust model and polynomial-fitting thrust model were in perfect agreement. This is an indication of mutual corroboration between the two advanced thrust models. The thrust-invariance assumption in the classical thrust model was not reasonable and overestimated the radial and tangential thrust accelerations.

In addition, an interesting mission scenario—the tour from earth to Vesta and Ceres using an electric sail with the analytical thrust model—was analyzed within an optimal framework using a hybrid direct optimization method. To reappraise the performance of the electric-sail-based spacecraft with the analytical advanced thrust model, trajectory optimizations with the classical thrust model were also implemented as a contrastive reference. The results showed that the transfer time using the electric sail with the advanced model was longer than that with the classical model. It is demonstrated that the decrease in performance between the classical and the advanced thrust model is related to the dimensionless propulsive acceleration modulus behavior.

REFERENCES

- [1] P. Janhunen
Electric sail for spacecraft propulsion
J. Propulsion Power, vol. 20, no. 4, pp. 763–764, 2004.
- [2] P. Janhunen
Increased electric sail thrust through removal of trapped shielding electrons by orbit chaotisation due to spacecraft body
Ann. Geophys., vol. 27, no. 8, pp. 3089–3100, 2009.
- [3] J. Siguier, P. Sarrailh, J. Roussel, V. Inguibert, G. Murat, and J. SanMartin
Drifting plasma collection by a positive biased tether wire in LEO-like plasma conditions: Current measurement and plasma diagnostics
IEEE Trans. Plasma Sci., vol. 41, no. 12, pp. 3380–3386, Dec. 2013.
- [4] P. Janhunen
Coulomb drag devices: Electric solar wind sail propulsion and ionospheric deorbiting
In *Proc. Space Propulsion Congr.*, pp. 1–8, 2014, Art. no. SP2014–2969331.
- [5] A. Kestilä *et al.*
Aalto-1 nanosatellite—Technical description and mission objectives
Geosci. Instrum. Methods Data Syst., vol. 2, pp. 121–130, 2013.
- [6] O. Khurshid, T. Tikka, J. Praks, and M. Hallikainen
Accommodating the plasma brake experiment on-board the Aalto-1 satellite
In *Proc. Nat. Acad. Sci. United States Amer.*, 2014, vol. 63, pp. 258–266.
- [7] P. Janhunen and A. Sandroos
Simulation study of solar wind push on a charged wire: basis of solar wind electric sail propulsion
Ann. Geophys., vol. 25, no. 3, pp. 755–767, 2007.
- [8] G. Mengali, A. A. Quarta, and P. Janhunen
Electric sail performance analysis
J. Spacecraft Rocket, vol. 45, no. 1, pp. 122–129, 2008.
- [9] P. Janhunen
The electric solar wind sail status report
In *Proc. Eur. Planetary Sci. Congr.*, vol. 5, pp. 1–2, 2010, Art. no. EPSC2010-297.
- [10] P. Janhunen, P. K. Toivanen, J. Polkko, S. Merikallio, P. Salminen, and E. Haeggström
Electric solar wind sail: Toward test missions
Rev. Sci. Instrum., vol. 81, no. 11, 2010, Art. no. 111301.
- [11] M. Huo, J. Zhao, S. Xie, and N. Qi
Coupled attitude-orbit dynamics and control for an electric sail in a heliocentric transfer mission
PLoS One, vol. 10, no. 5, 2015, Art. no. e0125901.
- [12] K. Yamaguchi and H. Yamakawa
Study on orbital maneuvers for electric sail with on–off thrust control
Aerosp. Technol. Japan, no. 12, pp. 79–88, 2013.
- [13] A. A. Quarta and G. Mengali
Minimum-time trajectories of electric sail with advanced thrust model
Aerosp. Sci. Technol., vol. 55, pp. 419–430, 2016.
- [14] M. Huo, G. Mengali, and A. A. Quarta
Electric sail thrust model from a geometrical perspective
J. Guid. Control Dyn., vol. 41, no. 3, pp. 734–740, 2018.
- [15] M. D. Rayman, T. C. Fraschetti, C. A. Raymond, and C. T. Russell
Dawn: A mission in development for exploration of main belt asteroids Vesta and Ceres
ACTA Astronautica, vol. 58, no. 11, pp. 605–616, 2006.
- [16] C. T. Russell *et al.*
Dawn arrives at Ceres: Exploration of a small, volatile-rich world
Science, vol. 353, no. 6303, pp. 1008–1010, 2016.
- [17] M. Huo, G. Mengali, and A. A. Quarta
Optimal planetary rendezvous with an electric sail
Aircraft Eng. Aerosp. Technol. vol. 88, no. 4, pp. 515–522, 2016.
- [18] D. Benson
A gauss pseudospectral transcription for optimal control
Ph.D. thesis, MA Inst. Technol., Cambridge, CA, USA, 2005.
- [19] P. Janhunen, A. A. Quarta, and G. Mengali
Electric solar wind sail mass budget model
Geosci. Instrum. Methods Data Syst., vol. 2, no. 1, pp. 85–95, 2013.



Mingying Huo received the Ph.D. degree in aeronautical and astronautical science and technology from Harbin Institute of Technology, Harbin, China, in 2015.

He is currently a Research Assistant with the Department of Aerospace Engineering, Harbin Institute of Technology, Harbin, China. His research interests include dynamics and control of electric solar wind sail, and shape-based trajectory optimization method.



Shilei Cao received the B.S. degree in aeronautical and astronautical science and technology from Harbin Institute of Technology, Harbin, China, in 2015. He is currently working toward the Ph.D. degree at the Department of Aerospace Engineering.

His research interests include electric solar wind sail and flexible space structures.



Yanfang Liu received the Ph.D. degree in aeronautical and astronautical science and technology from the Harbin Institute of Technology, Harbin, in 2014.

He has been a Lecturer with the Harbin Institute of Technology, where he is currently an Associate Professor with the Department of Aerospace Engineering. His research interests include smart materials and structures, nanopositioning, vibration isolation, unmanned aerial vehicles, and artificial intelligence.



He Liao received the Ph.D. degree in aeronautical and astronautical science and technology from the Harbin Institute of Technology, Harbin, in 2011.

He is currently a Senior Engineer with Shanghai Institute of Satellite Engineering. His research interests include overall design of satellite, non-linear Kalman filter, and electrostatic accelerometer.



Naiming Qi received the Ph.D. degree in precision instrument and machinery from Harbin Institute of Technology, Harbin, China, in 2001.

He is currently a Professor with the Department of Aerospace Engineering, Harbin Institute of Technology, Harbin, China. His research interests include dynamics and control of spacecraft and trajectory optimization method.